

# Investigation on Free Surface Flow Oscillatory Impact Pressures with the Volume of Fluid Method

Z. A. Sabeur      J. E. Cohen      J. R. Stephens  
*BMT Marine Information Systems Ltd, Southampton, UK*

A. E. P. Veldman  
*Department of Mathematics, University of Groningen, The Netherlands*

## 1 Introduction

The simulation of free surface flow within confined boundaries is an outstanding numerical problem in CFD because standard mathematical methods often lead to numerical instability when the fluid-air interface becomes ill-represented at the event of impact with a wall. However, recent attempts of modelling free surface flow with the volume of fluid method (VOF), by Sabeur *et al.* [5] and Veldman *et al.* [6], showed the possibility of modelling overturning waves with good numerical stability and representation of the free surface in contact with solid structures (Fig. 1).

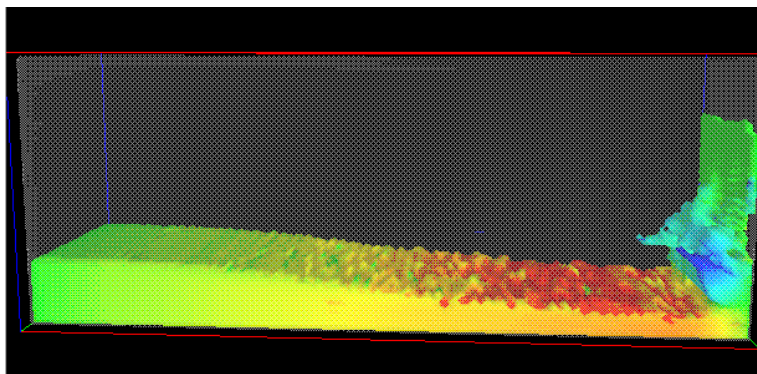


Figure 1: Three-dimensional dambreak simulation

In this paper, the theoretical prediction of short-time impact forces at boundaries made by Peregrine [3] is numerically investigated. These impact forces are of oscillatory nature and the order of a millisecond in duration. In Fig. 2, a sketch of the experimentally observed impact pressure is shown, and according to Peregrine the nature of the pressure oscillations could be caused by air bubble entrapment and oscillation within the flow at a confined boundary.

Also in Fig. 2, the impact pressure resulting from a VOF based numerical simulation ( $96 \times 48$  grid) is shown. As a result, the remarkable similarity between the two graphs led to questioning the origin of the pressure oscillations at impact, since air flow dynamics was not included in the VOF simulation. As a first measure to solve this problem, the authors required an accurate computation of the numerical impact oscillatory pressures at high grid resolution. Grid refinement at the region of impact was adopted and the resulting pressure time series processed accordingly.

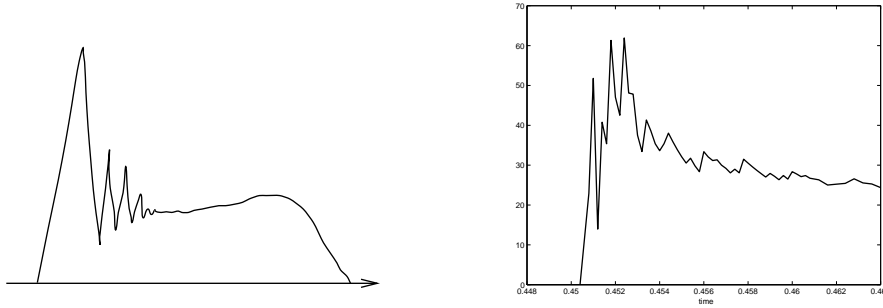


Figure 2: Oscillatory impact pressures as observed in experiments (*left*) and in numerical simulations (*right*)

## 2 Mathematical formulation

The general equations for fluid motion under transient conditions are given by the Navier–Stokes equations. In two dimensional Cartesian coordinates, they are given by the following differential equations:

$$\frac{\partial \rho}{\partial t} + \frac{\partial(\rho u)}{\partial x} + \frac{\partial(\rho v)}{\partial t} = 0, \quad (2.1)$$

$$\frac{\partial(\rho u)}{\partial t} + \frac{\partial(\rho u^2)}{\partial x} + \frac{\partial(\rho uv)}{\partial y} = \rho F_x + \sum_{r=x,y} \frac{\partial \sigma_{xr}}{\partial r}, \quad (2.2)$$

$$\frac{\partial(\rho v)}{\partial t} + \frac{\partial(\rho uv)}{\partial x} + \frac{\partial(\rho v^2)}{\partial y} = \rho F_y + \sum_{r=x,y} \frac{\partial \sigma_{yr}}{\partial r}. \quad (2.3)$$

$F_x$  and  $F_y$  represent the components of an external force field acting on the fluid,  $\sigma$  is the stress tensor and  $\rho$  is the density of the fluid. Further,  $u$  and  $v$  are the velocity field components in the  $x$  and  $y$  directions respectively and  $t$  is the time variable. In this study, the fluid is considered Newtonian and incompressible. Therefore, the fluid density  $\rho$  is considered constant in time and the stress tensor  $\sigma$  varies linearly with the fluid deformation rate. As a result, equations (2.1), (2.2) and (2.3) can be written in vectorial form as follows:

$$\text{div } U = 0, \quad (2.4)$$

$$\frac{\partial U}{\partial t} + (U \cdot \text{grad}) U = F - \text{grad } p + \nu \nabla^2 U. \quad (2.5)$$

$U$  and  $F$  are the velocity and external force vector fields respectively;  $p$  is the reduced pressure and  $\nu$  is the kinematic viscosity.

At the free surface, the continuity of normal and tangential stresses is enforced. A typical pressure equation at the free surface,  $p_{\text{fs}}$ , is given by

$$-p_{\text{fs}} + 2\nu \frac{\partial U_n}{\partial r_n} = -p_{\text{Air}} \frac{\rho_{\text{Air}}}{\rho} + \frac{2\gamma H}{\rho}, \quad (2.6)$$

supplemented with a condition on tangential stresses at the interface:

$$\nu \left( \frac{\partial U_n}{\partial r_t} + \frac{\partial U_t}{\partial r_n} \right) = 0. \quad (2.7)$$

$\gamma$  and  $H$  are the surface tension and mean curvature respectively;  $p_{\text{Air}}$  and  $\rho_{\text{Air}}$  are the reduced pressure and density of air;  $U_n$  and  $U_t$  are the normal and tangential velocities to the free surface.

### 3 Numerical model

**Equations of motion** Free surface flow VOF based models often discretize the Navier–Stokes equations in both time and space by means of finite-difference techniques. Eqs. (2.4) and (2.5) can be written as follows:

$$\operatorname{div} U^{n+1} = 0, \quad (3.1)$$

$$\frac{U^{n+1} - U^n}{\delta t} + \operatorname{grad} p^{n+1} = Q^n \equiv -(U^n \cdot \operatorname{grad}) U^n + \nu \nabla^2 U^n + F^n. \quad (3.2)$$

$\delta t$  is the time step and  $Q$  involves the finite-difference advective and diffusive terms and the external force  $F$ . The authors recommend Hirt and Nichols [2] for more details about the VOF method foundations and the adopted finite-difference discretisation scheme.

As indicated, the time integration is of explicit type, with automatically adjusted time step controlled by the CFL-number in a user prescribed range ( $0.2 < \text{CFL} < 0.5$ ).

**Free surface treatment** In the VOF method, a discrete function, the F-function, is used to indicate the fractional amount of fluid in each computational cell. A fluid tracking technique is used to advance the fluid in time. The technique operates through the classification of each computational cell type. Fluid cells are classified into seven categories: they include full, empty, free surface, degenerated, outflow, inflow and boundary cells. The displacement of the free surface should be such that mass is accurately conserved and artificial numerical droplets and bubbles avoided. In order to meet the latter criterion the original VOF method has been altered. The F-values at the free surface were transformed into a local height function  $h$ , with horizontal or vertical orientation. The free surface displacement is described by a local kinematic equation, which is solved by means of a finite-volume approach (Fig. 3 left).

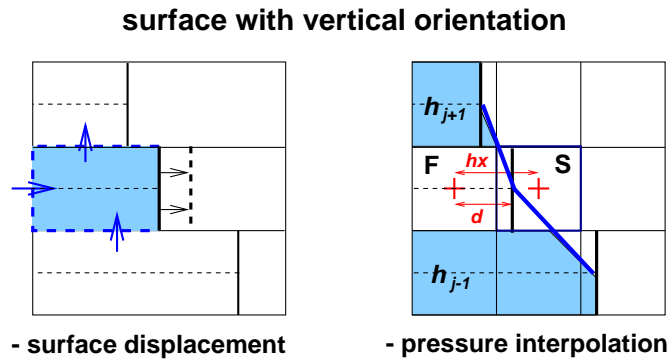


Figure 3: Displacement of the free surface (*left*) and interpolation of the pressure (*right*)

**Pressure condition** Free surface cells are provided with the normal-stress condition (2.6) which involves the orientation and curvature of the interface, the nearest pressure inside the fluid, the local atmospheric pressure at the free surface and surface tension. The curvature of the interface,  $H$  in (2.6), is computed from the local height function. The reduced pressure at the interface,  $p_{fs}$  in (2.6), is interpolated (or extrapolated) from the nearest dynamic pressure inside the fluid and normal to the interface (Fig. 3 right)

$$\frac{d}{hx} p_S + \left(1 - \frac{d}{hx}\right) p_F = p_{fs}. \quad (3.3)$$

**Poisson solver** Eqs. (3.1) and (3.2) lead to the Poisson equation (PE) for the pressure

$$\nabla^2 p^{n+1} = \text{div} \left( \frac{U^n}{\delta t} + Q^n \right). \quad (3.4)$$

A suitable solver for (3.4) greatly depends on the type of computer architecture available. Two types of solvers have been used in this study:

- an SOR solver with one-dimensional red-black ordering used on a 32 processor Cray J90 for hyperfine grid calculations;
- an MILU solver used on cache based RISC workstations and PC for preliminary coarse and medium grid calculations.

The SOR based method can run on a Cray J90 at 75% of the theoretical peak if all processor power is available [6]. Due to the boundary condition (3.3) the Poisson coefficient matrix can become non-symmetric, and no *a priori* predictions about the optimum relaxation factor can be made [4]. This factor is determined ‘on the fly’ by monitoring the rate of convergence, and following the technique developed by Botta and Ellenbroek [1].

As the pressure field at time level  $n + 1$  in equation (3.4) is computed, a new velocity field configuration is predicted by equation (3.2). This in turn advances the fluid in space, then enables to set the new type of fluid cells with their appropriate boundary conditions and finally updates the structure of the Poisson matrix for the next time level, and so on.

## 4 Impact pressures

Early theoretical studies by Peregrine [3] predicted the existence of short-time oscillatory wave impact pressures at a vertical wall (Fig. 2 left) and indicated that there was no upper limit to the magnitude of the pressure peaks. In this current work, we have pursued the above issues from a numerical point of view. A dambreak simulation, based on the VOF method, has been conducted. A cubic metre of water is suddenly released to a free fall in a 2.5m×1.25m rectangular tank and a fast moving wave front is generated to impact with the far end of the tank after approximately 0.45 s, see Fig. 4. The impact pressures have thus been evaluated at various locations along the tank wall.

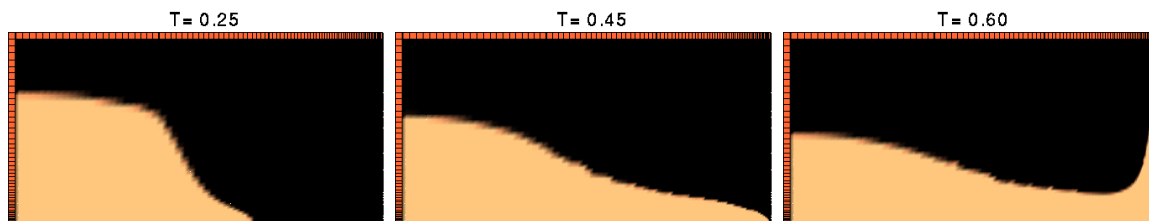


Figure 4: Snapshots of the fluid configuration in the dambreak simulation

The computations have been performed for various grid sizes, ranging from 96×48 to 1152×576. The grids are slightly stretched with refinement in the bottom far end corner of the tank. Most computations have been carried out for 0.5 s (*i.e.* shortly after impact). Table 1 gives an overview of the grids used, including details on local grid size, average time step and computational resources. The time indicated for the Cray J90 (peak 200

grid size	smallest mesh (m)	avg. time step (sec)	PE solver	computer	CPU time (total sec)
96×48	0.0064	0.67e-3	MILU	PC 200 MHz	75
192×96	0.0032	0.27e-3	MILU	PC 200 MHz	1050
384×192	0.0016	0.78e-4	SOR	Cray J90	9430
768×384	0.0008	0.39e-4	SOR	Cray J90	51800
1152×576	0.0005	0.20e-4	SOR	Cray J90	221400

Table 1: Overview of computations

Mflops/processor) refers to the total CPU time. Wall-clock time is much lower and depends on the number of parallel processors available.

Fig. 5 shows the impact pressure resulting from the simulations (apart from the 96×48 result shown in Fig. 2). The top row shows the pressure in the lower-right corner cell, *i.e.* at a point one half mesh size from the bottom. Note that this point moves towards the bottom with grid refinement. As this is not practical, the pressures have also been averaged over the lower inch space interval of the right hand wall (bottom row in Fig. 5).

The first observation on Fig. 5 suggests that the oscillatory nature of the pressure signals is present but without an apparent trend. Nevertheless, the pressure values in the lower right corner are more spiky than their corresponding averaged ones. The high peaks with pressure magnitudes over 100 are purely numerical since they appear as point like type of signals. These spikes can be removed immediately when a low-pass filter is used for processing the pressure time series data. This resulted into smoother curves for all grid refinements. The maximum value of the pressure peaks scales to values ranging between 70 and 100 reduced pressure units and between 60 and 80 for the averaged pressures.

As a consequence of the above, the Navier–Stokes equations will ideally predict non-oscillatory and smooth impact pressure signals with bounded peak values. This, however, suggests that air entrapment, induced in wave impact flows, may lead to an oscillatory regime of the resulting impact pressures.

## 5 Conclusion

An investigation about the origin of impact pressure oscillations at a vertical wall, generated in a dambreak flow simulation, has been carried out. There is evidence that the numerically observed impact pressure spikes, suggesting the existence of impact pressure oscillatory modes, should be attributed to numerical noise. A main pressure maximum persists and seems to scale to a stable value when finer grids are used in the VOF model simulations. Thus, further research is required in order to unravel the origin of the oscillatory impact pressures. These pressures are commonly observed in laboratory and field experiments and can only be investigated numerically when compressible air flow dynamics is included in the free surface flow models.

## References

- [1] E.F.F. Botta and M.H.M. Ellenbroek. A modified sor method for the Poisson equation in unsteady free surface flow calculations. *J. Computational Physics*, 60:119–134, 1985.

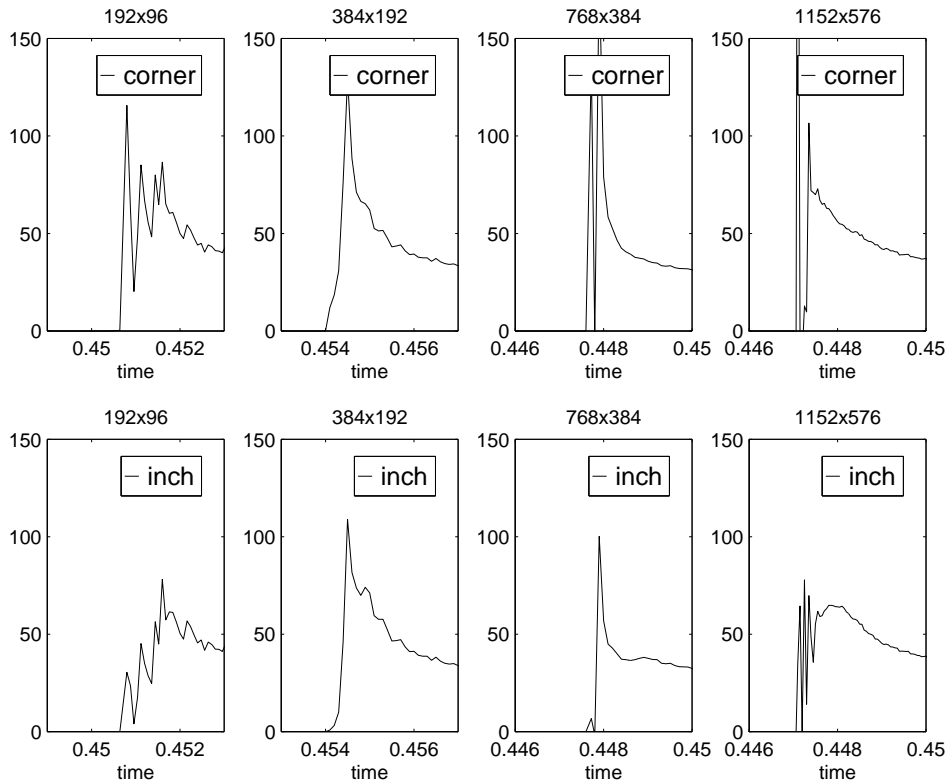


Figure 5: Pressure signals at impact in the right hand corner (*top row*) and corresponding averaged pressures (*bottom row*)

- [2] C.W. Hirt and B.D. Nichols. Volume of fluid method for the dynamics of free boundaries. *J. Computational Physics*, 39:201–225, 1981.
- [3] D.H. Peregrine. Pressures on breakwaters: A forward look. Mathematics Research Report AM-93-17, University of Bristol, UK, 1994.
- [4] Z.A. Sabeur. A parallel computation of the Navier-Stokes equations for the simulation of free surface flows with the volume of fluid method. In J. Dongara and J. Wasniewski, editors, *Applied Parallel Computing*, Lecture Notes in Computer Science 1041, pages 483–492. Springer Verlag, 1995.
- [5] Z.A. Sabeur, W. Roberts, and A.J. Cooper. Development and use of an advanced numerical model using the volume of fluid method for the design of coastal structures. In K.W. Morton and M.J. Baines, editors, *Numerical Methods for Fluid Dynamics V*, pages 565–573. Oxford University Press, 1995.
- [6] R.W.C.P. Verstappen and A.E.P. Veldman. Data-parallel solution of the incompressible Navier-Stokes equations. In P. Wesseling, editor, *High Performance Computing in Fluid Dynamics*, pages 237–260. Kluwer Academic Publishers, 1996.